INTERNATIONAL JOURNAL OF COMMUNICATION SYSTEMS
Int. J. Commun. Syst. 2013; **26**:1485–1499
Published online 12 March 2012 in Wiley Online Library (wileyonlinelibrary.com). DOI: 10.1002/dac.2326

A novel multicarrier CDMA transmission scheme for cognitive radios with sidelobe suppression

Morteza Rajabzadeh*,† and Hossein Khoshbin

Electrical Engineering Department, Ferdowsi University of Mashhad, Mashhad, Iran

SUMMARY

Noncontiguous multicarrier code division multiple access (MC-CDMA) is an effective multiple access method for cognitive radio systems that can deploy the noncontiguous vacant parts of a certain spectrum shared with the users of a primary system. However, the large spectral sidelobes of the Fourier transform based implementation of the MC-CDMA interfere with the adjacent primary transmission. In this paper, a novel complex signature sequence set is proposed for synchronous downlink MC-CDMA based cognitive radio networks to suppress the sidelobes. To do so, the minimization of the sidelobes power is developed as an eigen-optimization problem that is optimally solved by using the eigenvalue decomposition method. The optimal complex signature sequences are chosen as the eigenvectors attained by the eigenvalue decomposition of a symmetric matrix that is dependent of the spectral characteristics of the primary users. Simulation results show that by a slight decrease in the maximum number of active users compared with full load, the sidelobes can be considerably suppressed. The effect of cyclic prefix length, the bandwidth of the primary system and the number of active users on the sidelobe suppression performance is analyzed through numerical simulations.

Received 27 January 2011; Revised 16 January 2012; Accepted 16 January 2012

KEY WORDS: cognitive radio; MC-CDMA; sidelobe suppression; signature sequence design

1. INTRODUCTION

The increasing demand for high data rate wireless applications drives the efforts for more efficient usage of the finite natural radio spectrum resource. It is envisioned that this problem can be resolved through the utilization of cognitive radios (CRs) whose basic idea [1] covers many characteristics converting them to smart autonomous radios. Current requirements of wireless transmission and implementation challenges have highlighted some of these capabilities. Among them are the efficient secondary spectrum access and the shift from autonomous CR functioning to structured networking architectures, which is implied by IEEE 802.22 standard [2] and proposed in many works such as [3–5]. Multicarrier techniques such as OFDM and multicarrier code division multiple access (MC-CDMA) [6] are considered as promising candidates [7–10] for achieving the wide variety of CR application requirements, especially efficient secondary spectrum access.

In this paper, we have focused on developing a suitable MC-CDMA based transmission scheme for the cognitive radio networks. In the literature, two different transmission modes are proposed for the MC-CDMA based secondary networks: underlay [7, 11] and overlay [7, 8, 12, 13]. We have considered the overlay mode where the secondary MC-CDMA network is allowed to use a certain bandwidth shared with the users of a primary system such that minimum interference is made on primary users (PUs). Therefore, the secondary MC-CDMA must cease transmission on the subcarriers

*Correspondence to: Morteza Rajabzadeh, Electrical Engineering Department, Ferdowsi University of Mashhad, Mashhad, Iran.
†E-mail: morteza.rajabzade@gmail.com

located inside the PUs band and only deploy the remaining subcarriers. In this system, two important challenges arise. First, this system requires a set of signature sequences (i.e., spreading codes) that exist with any optional length because the number of remained data bearing subcarriers located in the allowed part of the spectrum can be any integer value. The deployment of orthogonal complex carrier interferometry (CI) signature sequences is the most important solution proposed for this purpose [7, 12, 13]. The second challenge is the intrinsic drawback of the Fourier based multicarrier techniques: power leakage because of the spectral sidelobes of the Fourier based MC implementation. Although the secondary transmitter deactivates the subcarriers located inside the band of the primary users, the spectral sidelobes of the adjacent data bearing subcarriers interfere with the transmission of the PUs. Deployment of sidelobe suppression techniques [14, 15] and migration to filterbank-based multicarrier system [16] are two dominant proposed solutions. The focal point of this paper is the former one. Several sidelobe suppression techniques are proposed in the literature for OFDM-based CR transmission. Deploying raised cosine window in time-domain slightly decreases the sidelobes with low complexity [17], but the OFDM symbol is lengthened. Therefore, it requires more cyclic prefix (CP) length and so the system throughput is decreased. In adaptive symbol transition (AST) [18] method, the OFDM symbol is extended by a data sequence designed based on the transmitted OFDM symbol. The AST method results in better sidelobe suppression performance compared with time-domain windowing. However, it suffers from the OFDM symbol lengthening. In subcarrier weighting (SW) approach [19], the data bearing subcarriers are weighted by a set of real-valued coefficients. There is no need for guardband tones in this approach. The weakness of SW is the degraded BER performance. The data tones can be precoded by orthogonal precoding vectors suggested for discrete Fourier transform (DFT)-based [20] and analog [21, 22] OFDM implementations. In the cancellation carrier (CC) [23, 24] and active interference cancellation (AIC) [15, 25] methods, the data symbols transmitted on the tones adjacent to the band occupied by the PUs are designed to suppress the interfering sidelobes. These methods provide good protection level to primary systems, but their main drawback is that the AIC (or CC) data must be calculated for each OFDM symbol separately. Hence, these methods are computationally expensive. Moreover, a remarkable part of the power in each OFDM symbol must be spent on the AIC (or CC) tones to provide moderate notches in the PU band.

The sidelobe suppression techniques mentioned above require that some sort of extra processing be added to the OFDM symbols. Although these methods are also applicable to MC-CDMA, we propose a novel sidelobe suppression scheme exclusively for MC-CDMA that provides an outstanding spectral notch in the PU band. In contrast to the available sidelobe suppression methods, this scheme deploys an inherent attribute of the MC-CDMA, the signature sequences, without the need for any extra redundancy or processing. For this purpose, the effect of the signature sequences on the frequency spectrum of the downlink MC-CDMA transmission has been analyzed and the leaked interfering sidelobes power on the PU band is introduced as the cost function to be minimized. This minimization is shown to be convertible to an eigen-optimization that is easily solved by eigenvalue decomposition (EVD) tool. The signature sequences are calculated as the eigenvectors corresponding to the smallest eigenvalues achieved by the eigenvalue decomposition of a symmetric matrix that is formed based on the spectral position of the primary users.

Simulation results show that by supporting less number of users with respect to the full load, the spectral sidelobes are remarkably suppressed, and reach almost zero. The decrement in maximum number of active users is very small and can be traded off for the required amount of the sidelobe suppression. Unlike the AIC , SW and AST methods that require recalculating the parameter used for sidelobe suppression (including the AIC tones, the coefficients, the mapping and the extended data) at *each* transmitted symbol, there is no need to recalculate the signature sequences for each transmitted MC-CDMA symbol, and the sequences are valid until the next spectral repositioning of the PUs. In addition, the problem of the sequences length being arbitrary is resolved by the proposed complex signature sequences. These complex sequences have the crucial orthogonality condition required for the MC-CDMA multiple access technique.

The paper is organized as follows. After introduction, downlink MC-CDMA system model is introduced considering both the DFT-based and analog implementation and its power spectrum is determined in Section 2. The eigen-optimization problem is developed in Section 3. Moreover, the

DOI: 10.1002/dac

signature sequences are designed to solve this problem. Performance evaluations and comparisons are considered in Section 4 by computer simulations. The paper is concluded in Section 5.

2. SYSTEM MODEL

We consider the downlink transmission of an unlicensed secondary system in a bandwidth that is shared with some licensed PUs. The secondary base station (BS) deploys MC-CDMA transmission/multiple access scheme to send data to K active secondary users by L subcarriers. Suppose that the data bits of the kth user are modulated with the rate $F_s = 1/T_s$. We denote the modulated data symbol at time slot n by $d_k(n)$that is spread by an $L \times 1$ signature sequence, $\mathbf{c}_k$. After adding the spread data vectors of all users, the $L \times 1$ frequency domain data vector is formed as

$$\mathbf{x}(n) = \sum_{k=1}^{K} \mathbf{c}_k d_k(n) = \mathbf{C}\mathbf{d}(n), \tag{1}$$

where $\mathbf{d}(n) = [d_1(n), d_2(n), \ldots, d_K(n)]^T$ is the $K \times 1$ vector containing the independent and identically distributed (i.i.d.) data symbols of different users. The matrix $\mathbf{C} = [\mathbf{c}_1, \mathbf{c}_2, \ldots, \mathbf{c}_K]$ is the $L \times K$signature sequence matrix of all active users, which is designed in the next section such that the sidelobes of the MC-CDMA frequency spectrum are minimized. The frequency domain data vector, $\mathbf{x}(n) = [x_0(n), x_1(n), \ldots x_{L-1}(n)]^T$, is passed to the OFDM modulator. Considering the addition of cyclic prefix, the complex envelope of the time domain MC-CDMA symbol has the form [22]

$$b(t) = \sum_{n=-\infty}^{\infty} \sum_{l=0}^{L-1} x_l(n) e^{j2\pi \frac{l}{T_s}(t-nT)} g_{\mathrm{TD}}(t - nT), \tag{2}$$

where $T = T_{\mathrm{cp}} + T_s$ is the length of an MC-CDMA symbol, T_{cp} is the duration of cyclic prefix and T_s is the length of the frequency domain data symbols such that $F_s = 1/T_s$ is the subcarrier spacing in the frequency domain. Also, $g_{\mathrm{TD}}(t)$ is the time domain pulse shaping filter that is assumed to be a rectangular pulse of length T for $t \in [-T_{\mathrm{cp}}, T_s)$. By considering the nth MC-CDMA frame, the Fourier transform of $b(t)$ becomes

$$B^{(n)}(f) = \sum_{l=0}^{L-1} x_l(n) a_l(f), \tag{3}$$

where

$$a_l(f) = T e^{-j\pi(T_s - T_{\mathrm{cp}})(f - l/T_s)} \mathrm{Sinc}\left(\pi T(f - l/T_s)\right). \tag{4}$$

In (4), the cardinal Sinc is defined as $\mathrm{Sinc}(x) = \sin(x)/x$. It can be seen that the Fourier transform of the analog transmission is the sum of phase shifted Sinc functions. The power spectral density (PSD) of (2) is given as

$$P_b(f) = \frac{1}{T} E\left\{ \left| B^{(n)}(f) \right|^2 \right\}. \tag{5}$$

In practice, MC transmission/reception is implemented in the discrete domain by inverse DFT (IDFT) and DFT modules. By deploying IDFT and CP insertion at the BS , the resultant discrete time domain samples constitute a block of length $M = L + \nu$ as follows:

$$y_m(n) = \frac{1}{\sqrt{L}} \sum_{l=0}^{L-1} x_l(n) e^{j2\pi(m-\nu)\frac{l}{L}}, \quad m = 0, 1, \ldots, M-1, \tag{6}$$

where ν is the CP length. The derivation of (6) is given in Appendix A. The time domain samples in (6) can be represented in an $M \times 1$ vector $\mathbf{y}^{(n)} = [y_0(n), y_1(n), \ldots, y_{M-1}(n)]^T$ as follows:

$$\mathbf{y}^{(n)} = \mathbf{F}^H \mathbf{D}\mathbf{x}(n). \tag{7}$$

DOI: 10.1002/dac

where $\mathbf{F}_{L\times M}$ is a discrete Fourier matrix with the (l,m)th entry $[F]_{l,m} = (1/\sqrt{L})e^{-j2\pi lm/L}$ and $\mathbf{D} = \text{diag}(1, e^{-j2\pi\nu/L}, \ldots, e^{-j2\pi\nu(L-1)/L})$ is an $L \times L$ diagonal matrix that models the CP addition.

By concatenating the MC-CDMA frames using parallel-to-serial conversion, the time domain data stream,

$$a_i = y_m(n), \tag{8}$$

is obtained where we have $i = nM + m$. Before frequency up-conversion, the baseband discrete time domain data stream, a_i, is passed through the analog-to-digital converter equipped with an interpolation filter $g_{\text{I}}(t)$. The resultant analog signal is expressed as

$$s(t) = \sum_{i=-\infty}^{\infty} a_i g_{\text{I}}(t - iT_0), \tag{9}$$

where T_0 denotes the sampling interval that is set as $T_0 = 1/L\Delta f$ for the subcarrier spacing of Δf. Compared with analog MC transmission, we have $T_0 = T_{\text{s}}/L$ [26]. The frame-based representation of $s(t)$ is

$$s(t) = \sum_{n=-\infty}^{\infty} \sum_{m=0}^{M-1} y_m(n) g_{\text{I}}(t - (nM + m)T_0). \tag{10}$$

Because MC-CDMA system is generally implemented by DFT modules, the sidelobe suppression techniques must be developed based on the spectral behavior of DFT based MC-CDMA as well. The power spectral density of analog baseband $s(t)$ in (10) is given by [26]

$$P_s(j\Omega) = \frac{1}{T_0} |G_I(j\Omega)|^2 \, E\left[\left|Y^{(n)}(j\Omega)\right|^2\right], \tag{11}$$

where

$$Y^{(n)}(j\Omega) = \sum_{m=0}^{M-1} y_m(n) e^{-jm\Omega T_0} = \frac{1}{\sqrt{L}} \sum_{m=0}^{M-1} \left(\sum_{l=0}^{L-1} x_l(n) e^{j2\pi(m-\nu)\frac{l}{L}} \right) e^{-jm\Omega T_0}. \tag{12}$$

This is in fact the sum of the spectrum of individual L subcarriers. Note that $Y^{(n)}(j\Omega)$ is a periodic function with period $2\pi/T_0$ because $x_l(n)$ is a discrete signal. The interpolation filter, $g_{\text{I}}(t)$, must be defined to be a lowpass filter with the cut-off frequency π/T_0. Hence, in the DFT-based MC transmission, the out-of-band spectral leakage is directly controlled by the spectral roll-off of $g_{\text{I}}(t)$. It is clear that frequency spectrum of $g_{\text{I}}(t)$ in the pass-band must be as flat as possible to not have any deteriorating effect on the in-band spectrum of $Y^{(n)}(j\Omega)$.

In our presumed CR scenario, the primary users transmit within the MC-CDMA spectrum (i.e., in the in-band). Therefore, we concentrate on the in-band spectrum of MC-CDMA that is characterized by $E\left[\left|Y^{(n)}(j\Omega)\right|^2\right]$. The in-band spectrum of L subcarriers lie in the frequency band of $[-(\pi/T_0), (\pi/T_0)]$. Hence, without loss of generality, we describe the continuous in-band spectrum of $[-(\pi/T_0), (\pi/T_0)]$ by the equivalent band of $[0, L-1]$ for ease of presentation of our sidelobe suppressing method. On the other hand, we upsample this band by a factor N_s to have a good spectral resolution (as in [15]). Therefore, the spectral spacing between two adjacent subcarriers (Δf) is represented by N_s samples. After upsampling, relation (12) can be rewritten as

$$Y_\gamma^{(n)} = \sum_{m=0}^{M-1} y_m(n) e^{-j2\pi m \frac{\gamma}{N_s L}}, \quad \gamma = 0, 1, \ldots, N_{\text{s}}L - 1. \tag{13}$$

The spectral samples, $Y_\gamma^{(n)}$, can be expressed in the vector form $Y_\gamma^{(n)} = \mathbf{e}_\gamma \mathbf{y}^{(n)}$ where $\mathbf{e}_\gamma$ is an $1\times M$ vector with the mth entry $e^{-j2\pi m(\gamma/N_s L)}$. The spectral samples are accumulated in an $N_{\text{s}}L \times 1$ vector $\mathbf{Y}^{(n)} = [Y_0^{(n)}, Y_1^{(n)}, \ldots, Y_{N_s L-1}^{(n)}]^T$ as follows:

$$\mathbf{Y}^{(n)} = \mathbf{E}\mathbf{y}^{(n)}, \tag{14}$$

DOI: 10.1002/dac

where the $N_s L \times M$ upsampled Fourier matrix, $\mathbf{E}$, is formed as $\mathbf{E} = [\mathbf{e}_0^T, \mathbf{e}_1^T, \ldots, \mathbf{e}_{N_s L-1}^T]^T$. Substituting (1) and (7) in (14), the upsampled spectrum of the DFT based MC-CDMA system becomes

$$\mathbf{Y}^{(n)} = \mathbf{E}\mathbf{F}^H \mathbf{D}\mathbf{C}\mathbf{d}(n). \tag{15}$$

In the next section, the signature sequence set for the proposed overlay based MC-CDMA cognitive radio network is proposed.

3. SIGNATURE SEQUENCE DESIGN

Assume that one PU deploys part of the in-band spectrum of the CR coinciding with subcarriers whose indices are in the set $I_{\text{PU}} = \{\mu_1, \mu_1 + 1, \ldots, \mu_2\}$, so the number of tones within the PU band is $N_{\text{PU}} = \mu_2 - \mu_1 + 1$. On each side of the primary transmission, λ subcarriers are considered as guard bands. The secondary base station should minimize the leaked power to the part of its band covering the subcarriers indexed as $I_{\text{PU-GB}} = \{\mu_1 - \lambda, \ldots, \mu_1, \mu_1 + 1, \ldots, \mu_2, \ldots, \mu_2 + \lambda\}$, which we call PU-GB band. Because there are $N_{\text{GB}} = 2\lambda$ guard band subcarriers, the number of the remaining subcarriers used for data transmission is $N_{\text{D}} = L - (N_{\text{PU}} + N_{\text{GB}})$. Clearly, the number of active users for the system to be fully loaded is $K_{\text{FL}} = N_{\text{D}}$ (FL denotes full load).

The MC-CDMA based cognitive radio must use the vacant parts of the available spectrum while not interfering on the band used by the primary system. The first solution for this goal is to deactivate the subcarriers located at the primary band. However, the spectral sidelobes of the adjacent data bearing subcarriers decay slowly. In this paper, it is proposed to design the signature sequence set of the active users such that the leaked power to the primary band because of the spectral sidelobes is suppressed.

The leaked power to the PU-GB band is denoted by the power of the spectral samples at this band. Let us denote the subset of indices of the upsampled spectrum within the PU and the guard band as $\Gamma_{\text{PU}}^{\text{GB}} = \{N_s(\mu_1 - \lambda), N_s(\mu_1 - \lambda) + 1, \ldots, N_s(\mu_2 + \lambda) - 1, N_s(\mu_2 + \lambda)\}$, which consists of $N_{\text{PU,GB}}^{\text{up}} = N_s(\mu_2 - \mu_1) + N_s(2\lambda) + 1$ samples. A new matrix, $\mathbf{E}_\Gamma$, is formed that is a submatrix of $\mathbf{E}$ containing those rows of $\mathbf{E}$ whose indices are in the set $\Gamma_{\text{PU}}^{\text{GB}}$. Clearly, the size of $\mathbf{E}_\Gamma$ is $N_{\text{PU,GB}}^{\text{up}} \times M$. Therefore, the spectral samples of the secondary transmission located at the PU and guard bands can be shown in the vector form as follows:

$$\mathbf{Y}_\Gamma^{(n)} = \mathbf{E}_\Gamma \mathbf{y}^{(n)} = \mathbf{E}_\Gamma \mathbf{F}^H \mathbf{D}\mathbf{C}\mathbf{d}(n). \tag{16}$$

Because the data vector $\mathbf{d}(n)$ is composed of random processes, the spectral samples in (16) are also random processes. Thus, the average leaked power to the PU-GB band can be obtained as

$$P_{\text{leaked}} = E\left[\left\|\mathbf{Y}_\Gamma^{(n)}\right\|_2^2\right] = E\left[\left\|\mathbf{E}_\Gamma \mathbf{F}^H \mathbf{D}\mathbf{C}\mathbf{d}(n)\right\|_2^2\right]. \tag{17}$$

Our problem is to determine the signature sequence set of the active users such that the leaked power to the PU-GB band is minimized. Thus, we formulate the problem at hand as the following constrained optimization problem:

$$\min_{\mathbf{C}} P_{\text{leaked}} = \min_{\mathbf{C}} E\left[\left\|\mathbf{E}_\Gamma \mathbf{F}^H \mathbf{D}\mathbf{C}\mathbf{d}(n)\right\|_2^2\right] \qquad \text{subject to } \mathbf{C}^H\mathbf{C} = \mathbf{I}_K, \tag{18}$$

where $\mathbf{I}_K$ is the $K \times K$ identity matrix. Note that the applied constraint makes the signature sequences orthogonal.

To solve the optimization problem in (18), we rewrite P_{leaked} as

$$P_{\text{leaked}} = E\left[\mathbf{d}^H(n)\mathbf{C}^H \mathbf{D}^H \mathbf{F}\mathbf{E}_\Gamma^H \mathbf{E}_\Gamma \mathbf{F}^H \mathbf{D}\mathbf{C}\mathbf{d}(n)\right]. \tag{19}$$

The above relation is in the form $P_{\text{leaked}} = E\left[\mathbf{b}^H(n)\mathbf{b}(n)\right]$ where $\mathbf{b}(n) = \mathbf{E}_\Gamma \mathbf{F}^H \mathbf{D}\mathbf{C}\mathbf{d}(n)$ is an $N_{\text{PU,GB}}^{\text{up}} \times 1$ vector. It is easy to investigate that $\mathbf{b}^H(n)\mathbf{b}(n) = \text{tr}\{\mathbf{b}(n)\mathbf{b}^H(n)\}$ where tr{.} is the linear

DOI: 10.1002/dac

trace operator [27], so P_{leaked} can be rephrased as

$$P_{\text{leaked}} = E\left[\text{tr}\left\{\mathbf{E}_\Gamma \mathbf{F}^H \mathbf{DCd}(n)\mathbf{d}^H(n)\mathbf{C}^H\mathbf{D}^H\mathbf{F}\mathbf{E}_\Gamma^H\right\}\right]. \tag{20}$$

The linear trace and expectation operators can be commuted as follows:

$$\begin{aligned} P_{\text{leaked}} &= \text{tr}\left\{E\left[\mathbf{E}_\Gamma \mathbf{F}^H \mathbf{DCd}(n)\mathbf{d}^H(n)\mathbf{C}^H\mathbf{D}^H\mathbf{F}\mathbf{E}_\Gamma^H\right]\right\} \\ &= \text{tr}\left\{\mathbf{E}_\Gamma \mathbf{F}^H \mathbf{DC}E\left[\mathbf{d}(n)\mathbf{d}^H(n)\right]\mathbf{C}^H\mathbf{D}^H\mathbf{F}\mathbf{E}_\Gamma^H\right\} \\ &= \text{tr}\left\{\mathbf{E}_\Gamma \mathbf{F}^H \mathbf{DCC}^H\mathbf{D}^H\mathbf{F}\mathbf{E}_\Gamma^H\right\}. \end{aligned} \tag{21}$$

In the above relation, note that the data symbols of different users are i.i.d. such that $E[\mathbf{d}(n)\mathbf{d}^H(n)] = \mathbf{I}_K$. Applying the fact that $\text{tr}\{\mathbf{TU}\} = \text{tr}\{\mathbf{UT}\}$ to (21), the constrained optimization problem in (18) is converted to

$$\min_{\mathbf{C}} P_{\text{leaked}} = \min_{\mathbf{C}} \text{tr}\left\{\mathbf{C}^H\mathbf{AC}\right\} \qquad \text{subject to } \mathbf{C}^H\mathbf{C} = \mathbf{I}_K, \tag{22}$$

where

$$\mathbf{A} = \mathbf{D}^H\mathbf{F}\mathbf{E}_\Gamma^H\mathbf{E}_\Gamma\mathbf{F}^H\mathbf{D} \tag{23}$$

is a symmetric $L \times L$ matrix. The above minimization problem is an eigen-optimization. The optimal solution is obtained by using one of the results of the Courant–Fisher minimax theorem [28]: For a given symmetric matrix such as $\mathbf{A}$ of dimension $L \times L$ and an arbitrary unitary matrix $\mathbf{C}$ of dimension $L \times K$ ($K \leqslant L$), the trace of $\mathbf{C}^H\mathbf{AC}$ reaches to its minimum (respectively maximum) when $\mathbf{C}$ is an orthogonal basis of the eigenspace of $\mathbf{A}$ associated with the algebraically smallest (resp. largest) eigenvalues. In particular, it is achieved for the eigenbasis itself. If eigenvalues are labeled increasingly and $\mathbf{u}_1, \ldots, \mathbf{u}_K$ are $L \times 1$ eigenvectors associated with the first K eigenvalues $\delta_1, \ldots, \delta_K$ and $\mathbf{U} = [\mathbf{u}_1, \mathbf{u}_2, \ldots, \mathbf{u}_K]$ with $\mathbf{U}^H\mathbf{U} = \mathbf{I}_K$ then,

$$\begin{cases} \min\limits_{\mathbf{C}} \text{tr}\left\{\mathbf{C}^H\mathbf{AC}\right\} = \text{tr}\left\{\mathbf{U}^H\mathbf{AU}\right\} = \delta_1 + \delta_2 + \ldots + \delta_K \\ \qquad\qquad \text{subject to } \mathbf{C}^H\mathbf{C} = \mathbf{I}_K. \end{cases} \tag{24}$$

This solution states that the minimized leaked power becomes the sum of the K smallest eigenvalues of $\mathbf{A}$. As a result, the minimized leaked power to the PU-GB band is a function of the distribution of eigenvalues of the matrix $\mathbf{A}$ and the number of active users. This dependency will be discussed in the simulation results section.

3.1. Discussions

The proposed scheme is applicable in the scenarios where a secondary BS is allowed to use the vacant parts of a frequency band while the users of a primary system have the license of using this band. For this purpose, multicarrier transmission techniques have shown to be good candidates. The secondary BS should deploy a multiple access scheme to send the data to different users. The multicarrier code division multiple access is a good solution providing both the multicarrier transmission and multiple access functionalities. Besides, the secondary BS can minimize the leaked transmitted power to the adjacent bands used by the primary users by utilizing the proposed signature sequences.

The design of the signature sequences can be summarized as follows. Upon obtaining the information of the parts of the spectral band used by the primary system, the secondary base station builds the matrix $\mathbf{E}_\Gamma$ so that the leaked power to spectral band of the PU and the assigned guard interval can be calculated. Then, the symmetric matrix $\mathbf{A} = \mathbf{D}^H\mathbf{F}\mathbf{E}_\Gamma^H\mathbf{E}_\Gamma\mathbf{F}^H\mathbf{D}$ is formed. The minimization in (24) requires solving a standard eigenvalue problem after which the eigenvectors corresponding to K smallest eigenvectors are allocated as the signature sequences of K active users. In (24), the optimal $\mathbf{C}$ is not unique, because any system $\mathbf{C}$ that is an orthonormal basis of the eigenspace associated with the first K eigenvalues will be optimal. In this manner, the eigen problem is only solved

DOI: 10.1002/dac

at the BS and the signature sequences are sent to the users by a signaling channel. Hence, there is no computational burden on the secondary users.

The calculation of EVD of an $L \times L$ matrix is the most computationally demanding part of the problem solution. The complexity order of such EVD calculation is $O(L^3)$ [29]. The complexity of the method is independent of the spectral environment. The designed signature sequences are sent to the users by the signaling channel, and they are valid until the next spectral displacement of the primary users. This is one of the advantages of the proposed sidelobe suppression method over the AIC and CC methods [15, 23–25] and also AST method [18] because in these methods, the data of AIC tones and the AST data should be updated at every sent MC-CDMA frame. The update of AIC (or CC) tones involves solving a least-squares problem.

The pattern of the spectrum usage by the primary users may be changed. When the base station of the CR becomes aware of the changes, it must adapt itself to the new spectral environment. Thus, the BS recalculates the new signature sequences and sends them to the secondary users. If the spectral displacement of the primary users occurs very often, the signature sequence set must be updated frequently to deploy only the vacant subcarriers and suppressing the leaked sidelobe power to the PUs band. The frequent need for update of the sequences increases the transmission delay and the computational requirements. In fact, these issues are the natural challenges that lie ahead of implementation of the cognitive radio networks. For example, the implementation of precoders for sidelobe suppression in multicarrier systems [20, 21] and the deployment of cooperative spectrum sensing approaches [30] encounter similar challenges in the environments that alter frequently. Therefore, the signature sequence set is favorable in the situations where the spectral displacement rate of the primary users is slow to moderate. For example, it is applicable for the situations similar to the IEEE 802.22 where the primary users' channels (TV channels) do not often change.

It is important to note that the proposed signature sequence set is mainly designed to provide low spectral sidelobes in the in-band primary transmission while satisfying the orthogonality of the sequences. Because the downlink transmission is considered to be synchronous, the optimal zero-lag cross-correlation constraint is sufficient for the designed sequence set [31] that is fully satisfied by the $\mathbf{C}^H\mathbf{C} = \mathbf{I}_K$ constraint. Although the proposed approach for signature sequence design is developed based on the DFT based implementation of the MC-CDMA system, the development of the approach for analog implementation is straightforward. It suffices to use the power spectrum of the analog implementation (i.e., $B^{(n)}(f)$ in (3)) instead of the power spectrum of the DFT based implementation (i.e., $Y^{(n)}(j\Omega)$ in (12)) to derive the relations in this section.

In the next section, it is shown that signature sequences designed in (24) provide deep notches in the PU-GB band and make the frequency spectrum of the MC-CDMA transmission be noncontiguous. Therefore, the proposed transmission scheme is called NC-Eigen MC-CDMA or NC-EIG for short.

3.2. Receiver of the secondary users

After the signature sequence set is updated, the secondary BS informs each of the users of its new signature sequence. Then the BS starts the data transmission utilizing the new signature set matrix that is updated based on the solution of the eigen problem provided in (22). Consider the transmitted frequency domain signal vector in (1). At the receiver of the desired user (e.g., mth user), after CP removal and DFT processing, the received $L \times 1$ frequency domain signal vector can be expressed as

$$\mathbf{r}_m = \mathbf{H}_m \sum_{k=1}^{K} \mathbf{c}_k d_k + \boldsymbol{\zeta}_m = \mathbf{H}_m \mathbf{c}_m d_m + \mathbf{H}_m \sum_{\substack{k=1 \\ k \neq m}}^{K} \mathbf{c}_k d_k + \boldsymbol{\zeta}_m \tag{25}$$

in which $\mathbf{H}_m$ is an $L \times L$ diagonal matrix whose (l, l) entry is equal to the lth DFT coefficient of the impulse response of the communication channel between the secondary BS and the mth user. Also, $\boldsymbol{\zeta}_m$ is the complex additive white Gaussian noise vector with zero mean and covariance matrix $\mathbf{R}_{\boldsymbol{\zeta}} = \sigma_{\zeta}^2 \mathbf{I}_L$. Another advantage of the proposed scheme is that no extra processing is required at the receiver of the secondary radio network to fulfill the spectrum sharing tasks. The receiver should

DOI: 10.1002/dac

only equalize the communication channel and despread the data before the demodulation process. Any channel equalization scheme can be used at the receiver. We simply use the inverse of the channel matrix to undo the channel effect [32]. Thus, after the equalization, relation (25) becomes

$$\hat{\mathbf{r}}_m = \mathbf{H}_m^{-1}\mathbf{r}_m = \mathbf{c}_m d_m + \sum_{\substack{k=1 \\ k\neq m}}^{K} \mathbf{c}_k d_k + \mathbf{H}_m^{-1}\boldsymbol{\zeta}_m. \tag{26}$$

The applied constraint in the optimization ($\mathbf{C}^H\mathbf{C} = \mathbf{I}_K$) makes the designed signature sequences mutually orthonormal. It means that we have: $\mathbf{c}_m^H\mathbf{c}_k = \delta(m-k)$. Hence, after despreading we have

$$\hat{d}_m = \mathbf{c}_m^H\mathbf{H}_m^{-1}\mathbf{r} = d_m + \mathbf{c}_m^H\left(\sum_{\substack{k=1 \\ k\neq m}}^{K} \mathbf{c}_k d_k + \mathbf{H}_m^{-1}\boldsymbol{\zeta}_m\right) = d_m + \mathbf{c}_m^H\mathbf{H}_m^{-1}\boldsymbol{\zeta}_m. \tag{27}$$

It is seen that multiuser interference is fully mitigated because of the orthogonality of the signature sequence set.

4. SIMULATION RESULTS AND COMPARISONS

In this section, we conduct simulations to evaluate the performance of the proposed MC-CDMA transmission scheme. Consider an MC-CDMA base station that has the privilege to transmit data to K secondary users in a cognitive radio scenario utilizing a bandwidth of $L\Delta f$ where Δf is the subcarrier spacing. The number of subcarriers is assumed to be $L = 128$, and the CP length is $\nu = 16$. A sequence of independent, identically distributed symbols with 16QAM modulation is sent from the base station to each user. The upsampling factor is assumed to be $N_s = 8$. In the results demonstrated below, the averaged power spectra are obtained from 5000 simulation runs.

As the reference, we have considered the noncontiguous carrier interferometry (NC-CI) MC-CDMA where the subcarriers located in the PU transmission and guard subcarriers are turned off [12]. In this situation, the CI codes length is N_D and the maximum number of orthogonal users becomes $K_{FL} = N_D$. Note that because the number of remaining data subcarriers (N_D) may be any integer value, we require the signature sequences that exist with any arbitrary length. The CI sequences are complex orthogonal sequences that possess this property. It has been shown that their error performance is the same as orthogonal Hadamard–Walsh sequences [12, 13].

Suppose one PU transmission is present at part of the available band coinciding with subcarriers $\#v_1 = 51$ to $\#v_2 = 70$; that is, $(N_D, N_{PU}, 2\lambda) = (108, 20, 0)$. In Figure 1, we have depicted the normalized power spectral density of our proposed eigen-based MC-CDMA transmission (NC-EIG) for different number of active users. The power spectral density of noncontiguous carrier interferometry MC-CDMA (shortly, NC-CI) is also shown. The vertical lines denote the borders of PU band. In this paper, the maximum value of the spectral sidelobes at the PU band is chosen as the performance metric that is demonstrated by a horizontal line for each of the curves. The line types are dotted and solid for the NC-CI and NC-EIG transmission schemes, respectively. It can be seen that NC-CI has the highest sidelobes in the PU band that is almost independent of the number of its users, so deactivation of the tones in the PU band is not effective to avoid interfering with the adjacent primary users. For the proposed NC-EIG scheme, it can be seen that its sidelobe suppression ability is related to the number of active users. In the full load case ($K = N_D = 108$), no considerable performance improvement is seen compared with NC-CI. By decreasing the number of active users to $K = 98$, the spectral sidelobe power is reached beneath –90 dB, which is an acceptable value in practical systems [14]. Although the spectral sidelobe values smaller than –90 dB are negligible, the normalized PSD of the NC-EIG for lesser number of active users is also depicted. For $K < 93$, the sidelobe suppression is maintained almost unchanged at a minimum level. To analyze this observation, we may have a look at (24) where it is evident that in NC-EIG scheme, the leaked power to the PU band is the sum of the K smallest eigenvalues of the matrix $\mathbf{A}$. Therefore, we use the non-normalized cumulative sum of eigenvalues (NNCSE) of $\mathbf{A}$ as a good indicator of the performance of NC-EIG, which is

DOI: 10.1002/dac

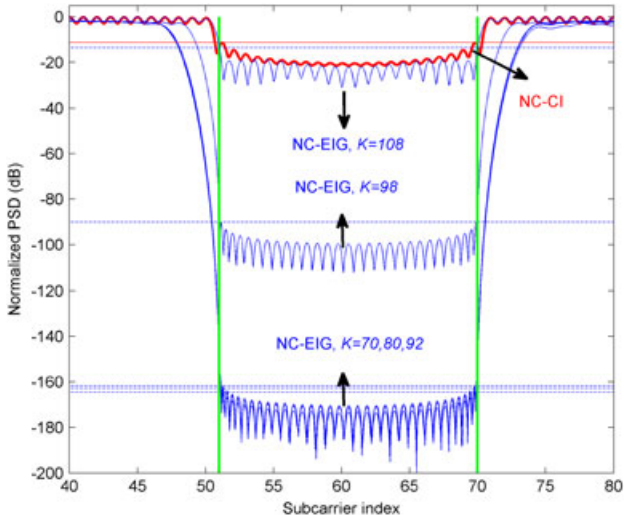

Figure 1. Normalized power spectrum for $(N_D,N_{PU},2\lambda)$=(108,20,0).

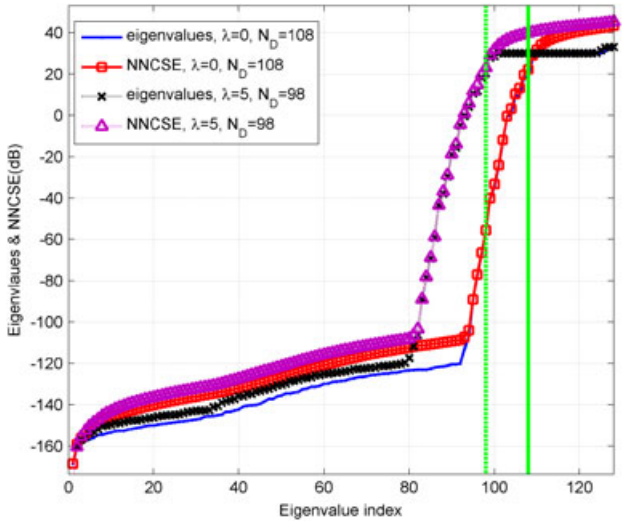

Figure 2. Eigenvalues of the matrix **A** for two scenarios: $(N_D, N_{PU}, 2\lambda) = (108, 20, 0)$ and $(N_D, N_{PU}, 2\lambda) = (98, 20, 10)$.

defined as NNCSE$(K) = \delta_1 + \delta_2 + \ldots + \delta_K$ for $K \in \{1, \ldots, L\}$(The cumulative sum of eigenvalues is a widely used tool in principal component analysis [27] to assess the 'practical' dimensionality of a correlation matrix). For the scenario in Figure 1 (i.e.,$(N_D, N_{PU}, 2\lambda) = (108, 20, 0)$), the eigenvalues of **A** are shown in Figure 2 by the dotted curve. The graph of NNCSE values versus number of users is also depicted by the circled curve (both in dB). The sidelobe suppression performance of NC-EIG can be easily justified by this figure. The vertical solid line is located at the index N_D. It can be seen that the first 92 eigenvalues are very small (below –120 dB) and after that they are gradually increased. The last $(N_{PU} + 2\lambda)$ eigenvalues are largest and almost equal. This trend is reasonably followed in the NNCSE. In a trade-off between increasing the number of active users (to increase the system capacity) and decreasing the spectral sidelobe on the PU band (to decrease NNCSE), it is reasonable to set $K \leqslant K^{\text{trade-off}} = 92$. Because at this index, on the one hand, NNCSE starts to increase (we call this index start-to-increase index) and on the other hand, the achieved sidelobe suppression is very good (about –160 dB, based on Figure 1). By increasing $K$from 92 to $N_D = 108$, the sidelobe suppression performance is degraded, and for $K = N_D = 108$, the sidelobe suppression performance is almost the same as NC-CI.

DOI: 10.1002/dac

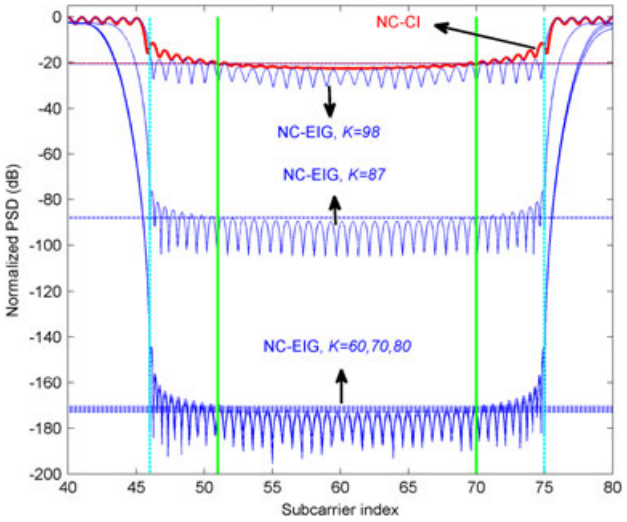

Figure 3. Normalized power spectrum when (N_{D},N_{PU},2λ)=(98,20,10).

To analyze the dependency of the sidelobe suppression performance to the guard band size, the eigenvalues and the NNCSE curves are shown in Figure 2 for the scenario with $\lambda = 5$ guard band tones (i.e.,$(N_{\mathrm{D}}, N_{\mathrm{PU}}, 2\lambda) = (98, 20, 10)$) by the curves with specifiers '+' and square, respectively. It is seen that by inserting guardbands, NC-EIG encounters a larger barred spectral band. This decreases the number of very small eigenvalues. The vertical dashed line is located at the index N_{D} for this scenario. In this scenario, the start-to-increase index of the NNCSE curve is decreased to 78 (compared with the previous index 92). Therefore, increasing the number of guardband tones does not have much effect on the ultimate sidelobe suppression ability of the NC-EIG. On the other hand, it decreases the number of users that is traded-off between capacity and sidelobe suppression to $K^{\text{trade-off}} = 78$. Note that the NNCSE represents the overall leaked power to the PU-band. The performance criterion depicted in Figure 1 is the peak of the sidelobes of the normalized PSD in the PU-band that is more suitable. As can be seen in Figure 1, for example for $K = 98$, the peaks of sidelobes in the PU band occur in the band edges. Consequently, although increasing the number of guardband tones does not have much effect on the ultimate sidelobe suppression ability of the NC-EIG, a few guard band tones are necessary for the NC-EIG to reach its best performance in the PU band. This feature is illustrated in Figure 3 where the normalized PSD of the NC-CI and NC-EIG transmission schemes are depicted for the second scenario ($\lambda = 5$). The vertical dashed lines indicate the guardband borders. It can be seen that the presence of guardband lets the sidelobes reach their minimum value at the PU bands. For example, when $K = 70$, the peak value of spectral sidelobes is about 10 dB smaller compared with the sidelobes for $K = 70$ in Figure 1 (with $\lambda = 0$). However, for $\lambda = 5$, $K^{\text{trade-off}}$ is decreased from 92 to 78, which is concluded based on the reasoning presented for Figure 2. In the remaining part of this section, we consider the number of guardband tones to be $\lambda = 2$ at each side of the PU band.

Increase of the CP length generally decreases the sidelobe suppression performance of the MC sidelobe suppression methods (e.g., the CC method [24]). The effect of the cyclic prefix length on the sidelobe suppression performance of NC-EIG is demonstrated in Figure 4 for the scenario of Figure 1. When the CP length increases, the dominant effect is that the start-to-increase index of the eigenvalues is reduced. Nonetheless, the very small region of the eigenvalues curve is maintained. This means that for higher CP lengths, the ultimate sidelobe suppression capability of the NC-EIG is preserved, but it is reached with a decreased traded-off value of the maximum number of users.

The CR may encounter situations where a PU with large bandwidth or multiple spectrally disjoint PUs start to deploy some parts of the shared spectrum. To analyze the applicability of the proposed approach in such circumstances, two new scenarios are considered. First, it is assumed that each of two spectrally-disjoint primary users utilize the spectral bandwidth covering 20 subcarriers

DOI: 10.1002/dac

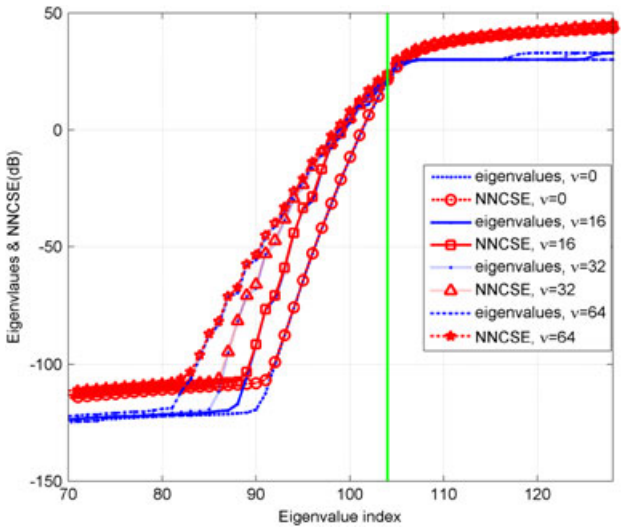

Figure 4. Eigenvalues of the matrix **A** for different number of CP lengths when $(N_{\mathrm{D}},N_{\mathrm{PU}},2\lambda)$=(108,20,0).

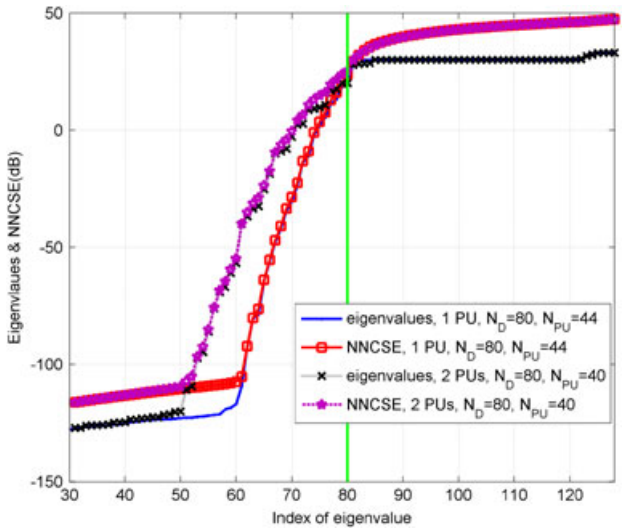

Figure 5. Eigenvalues of the matrix **A** for two narrowband spectrally-disjoint PUs and a large bandwidth PU.

of the CR system, so we have: $(N_{\mathrm{D}}, N_{\mathrm{PU}}, N_{\mathrm{GB}}) = (80, 40, 8)$. Second, a single PU with larger bandwidth requirement is assumed that its bandwidth covers 44 subcarriers of the CR band (i.e., $(N_{\mathrm{D}}, N_{\mathrm{PU}}, N_{\mathrm{GB}}) = (80, 44, 4)$). The zoomed plots of eigenvalues and NNCSE for these scenarios are shown in Figure 5. The number of barred tones ($N_{\mathrm{PU}}^{\mathrm{GB}} = N_{\mathrm{PU}} + N_{\mathrm{GB}} = 48$) and also the number of remaining data tones ($N_{\mathrm{D}} = 80$) are equal for both scenarios. From this figure, it is clear that the distribution of the $N_{\mathrm{PU}}^{\mathrm{GB}}$ larger eigenvalues is quite the same for both scenarios. Moreover, the NC-EIG scheme is able to suppress its sidelobes to the very low level for both scenarios. The only difference is that in the case of encountering one PU with large bandwidth, eigenvalues are more rapidly reduced to the region of very small values, so for this scenario, the traded-off number of users is $K^{\text{trade-off}} = 60$. But in the first scenario, the NC-EIG can efficiently suppress its sidelobe with a lower value of the traded-off number of users, that is, $K^{\text{trade-off}} = 50$. This discussion is confirmed by the normalized power spectral densities of these scenarios illustrated in Figures 6 and 7, respectively.

DOI: 10.1002/dac

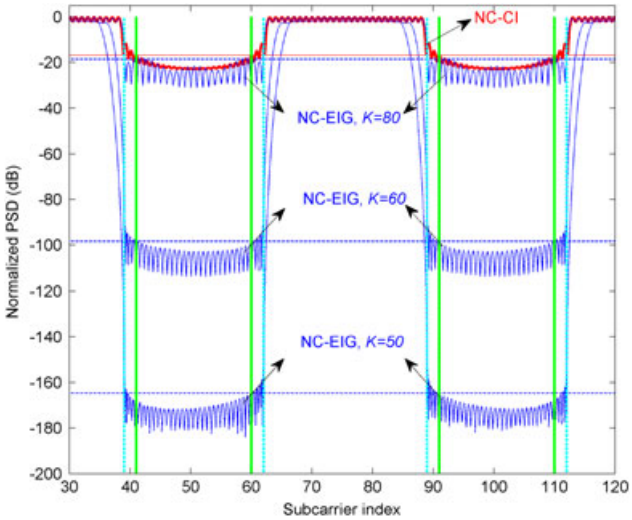

Figure 6. Normalized power spectrum for two narrowband spectrally-disjoint primary users.

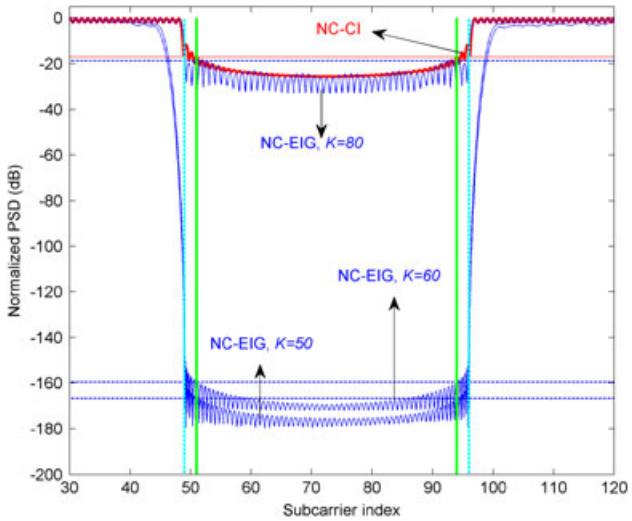

Figure 7. Normalized power spectrum for a large bandwidth primary user.

The solution of the eigen-optimization in (24) shows that by deploying the proposed signature sequences, the minimum leaked power to the PU-GB band is the sum of the K smallest eigenvalues of matrix $\mathbf{A}$. Because the distribution of eigenvalues of $\mathbf{A}$ directly controls the leaked power to the spectral band of primary users, let us discuss their distribution. If the frequency spectrum is not upsampled (i.e., $N_s = 1$), the size of $\mathbf{E}_\Gamma$ will be $(N_{\mathrm{PU}} + N_{\mathrm{GB}}) \times M$ and we have $\mathrm{rank}[\mathbf{A}] = (N_{\mathrm{PU}} + N_{\mathrm{GB}})$. Consequently, N_D eigenvalues of $\mathbf{A}$ will be zero. However, without upsampling, the optimization in (24) will zero out the spectral interference on only the center frequencies of the subcarrier tones located in the PU-GB band. This does not guarantee good sidelobe suppression in the frequency spacings between these center frequencies. By upsampling the region between subcarrier tones by a factor N_s(determined such that a good resolution is provided [15, 22]), the overall interference on the PU-GB band is considered in the matrix $\mathbf{A}$ with a good approximation. The effect of upsampling on the eigenvalues of $\mathbf{A}$ is the reduction of the number of zero eigenvalues from N_D to start-to-increase index (which we have chosen as $K^{\text{trade-off}}$). Besides, the $(N_{\mathrm{PU}} + N_{\mathrm{GB}})$ large eigenvalues are preserved. The remaining eigenvalues are gradually increased from the very small values to the large eigenvalues (that is the roll-off region in the Figures 2, 4 and 5). If the secondary BS lets the maximum number of active users be equal to the number of zero eigenvalues

DOI: 10.1002/dac

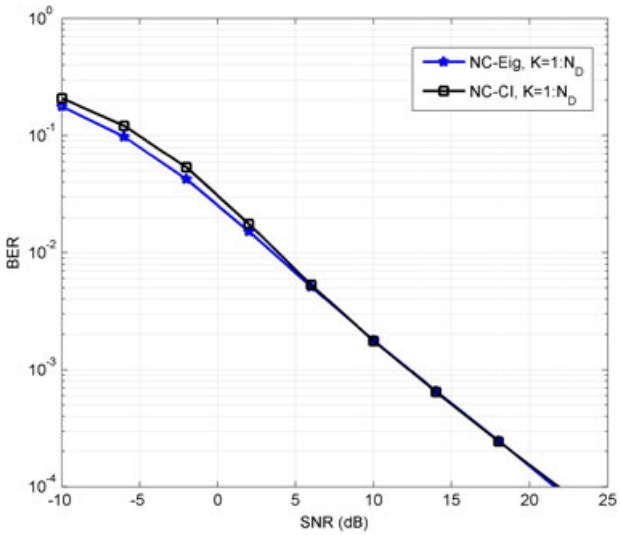

Figure 8. Bit error rate versus signal-to-noise ratio for (N_{D},N_{PU},2λ)=(108,20,0).

($K = K^{\text{trade-off}}$), the interference on the PU-GB band will be very small (nearly zero). Simulation results show that the value of $K^{\text{trade-off}}$ is slightly smaller than the number of $K_{\mathrm{FL}} = N_{\mathrm{D}}$), and it is a function of CP length, the bandwidth and the number of primary users. In practical applications, the desired amount of sidelobe suppression is not required to be zero. On the basis of the desired amount of the sidelobes suppression, more users (with respect to $K^{\text{trade-off}}$) can be supported by the secondary BS. For example, in Figure 1, we have $K^{\text{trade-off}} = 92$. However, if the sidelobe suppression of –90 dB is enough, $K = 98$ users can be supported. Note that fully-loaded number of active users is $K_{\mathrm{FL}} = N_{\mathrm{D}} = 108$. Hence, the proposed NC-EIG scheme for CR NC-MC-CDMA transmission achieves a very good level of sidelobe suppression with just a little decrease in the capacity. Moreover, the secondary BS can easily control the amount of interfering leaked power on the PU band by varying the number of active users.

The BER performances of NC-EIG and NC-CI are shown in Figure 8 versus signal-to-noise ratio for the PU transmission scenario of Figure 1. The frequency selective channel between the base station and each user has been realized based on an exponential power delay profile with $L_c = 16$ resolvable paths where the exponential decay factor is assumed to be $\beta = 0.1$. It can be seen that the NC-EIG is able to completely eliminate multiuser interference because based on the receiver structure described in Section 3, the channel effect is eliminated and also the signature sequences attained by the eigen-optimization in (24) are orthogonal. Therefore, the orthogonality between user signatures are preserved in synchronous downlink transmission and each receiver is able to completely reject multiuser interference. Because the error performance of the CI codes is the same as Hadamard–Walsh codes [13], the designed signature sequences can achieve error performances similar to orthogonal binary Hadamard–Walsh codes.

5. CONCLUSIONS

In this paper, we have developed a downlink MC-CDMA based secondary network that is allowed to transmit in a specific spectrum shared with a primary system. To suppress the interfering effect of the spectral sidelobes of the MC-CDMA transmission, a novel approach is proposed to calculate the signature sequences of the active users based on solving an eigen-optimization problem. The achieved sidelobe suppression mainly depends on the number of active users. By accepting a slight decrease in the maximum number of active users (with respect to full load), the spectral sidelobes on the PU band are significantly reduced to almost zero. Therefore, the secondary base station can apply a trade-off between the required sidelobe suppression level on the PU band and the system capacity (in terms of number of active users). The designed signature sequences are orthogonal and can effectively treat the multiuser interference. The signature sequences must be updated when the

DOI: 10.1002/dac

pattern of the spectrum usage of the primary system is changed. Thus, this method is beneficial in the environments where the spectral displacement of the primary users is slow to moderate.

6. APPENDIX A

Suppose the frequency domain data symbols, $x_l(n)$, are passed through the IDFT block. The samples at the output of IDFT are given as

$$z_\mu(n) = \frac{1}{\sqrt{L}} \sum_{l=0}^{L-1} x_l(n) e^{j2\pi \frac{\mu l}{L}}, \quad \mu = 0, \ldots, L-1. \tag{A.1}$$

To insert the CP , the last ν samples of $z_\mu(n)$ are inserted at the beginning of the data stream in (A.1). Let us consider these samples as $v_\lambda(n) = z_{L-\nu+\lambda}(n)$ for $\lambda = 0, \ldots, \nu-1$ that can be written as

$$v_\lambda(n) = z_{L-\nu+\lambda}(n) = \frac{1}{\sqrt{L}} \sum_{l=0}^{L-1} x_l(n) e^{j2\pi \frac{l}{L}(L-\nu+\lambda)}. \tag{A.2}$$

The relation (A.2) can be rephrased as

$$v_\lambda(n) = \frac{1}{\sqrt{L}} \sum_{l=0}^{L-1} x_l(n) e^{j2\pi l} e^{j2\pi \frac{l}{L}(-\nu+\lambda)} = \frac{1}{\sqrt{L}} \sum_{l=0}^{L-1} x_l(n) e^{j2\pi \frac{l}{L}(\lambda-\nu)}. \tag{A.3}$$

Therefore, in (6), the last L samples are the output of the IDFT block and the first ν samples are the inserted cyclic prefixes.

ACKNOWLEDGEMENTS

This work was supported in part by the Iranian Research Institute for ICT (ITRC).

REFERENCES

1. Mitola J. Cognitive radio for flexible mobile multimedia Communications. *International Workshop on Mobile Multimedia Communications*, 1999; 3–10.
2. IEEE 802 LAN/MAN Standards Committee 802.22 WG on WRANs (Wireless Regional Area Networks) IEEE 802 LAN/MAN Standards Committee, Piscataway, NJ [Online]. Available: http://www.ieee802.org/22/.
3. Attar A, Nakhai MR, Aghvami AH. Cognitive radio transmission based on direct sequence MC-CDMA. *IEEE Transactions on Wireless Communications* 2008; **7**(4):1157–1162.
4. Wang R, Lau VKN, Lv L, Chen B. Joint cross-layer scheduling and spectrum sensing for OFDMA cognitive radio systems. *IEEE Transactions on Wireless Communications* 2009; **8**(5):2410–2416.
5. Ngo DT, Tellambura C, Nguyen HH. Resource allocation for OFDMA-based cognitive radio multicast networks with primary user activity consideration. *IEEE Transactions on Vehicular Technology* 2010; **59**(4):1668–1679.
6. Ko K, Woo C. Effects of carrier frequency offset on the average effective SNR and the average BER for asynchronous MC-CDMA uplink systems with a guard period. *International Journal of Communication Systems* 2011; **24**(12):1565–1583.
7. Chakravarthy V, Li X, Wu Z, Temple MA, Garber F, Kannan R, Vasilakos A. Novel overlay/underlay cognitive radio waveforms using SD-SMSE framework to enhance spectrum efficiency - Part I: theoretical framework and analysis in AWGN channel. *IEEE Transactions on Communications* 2009; **57**(12):3794–3804.
8. Sarath D, Nolan KE, Sutton PD, Doyle LE. Exploring the reconfigurability options of multi-carrier CDMA in cognitive radio systems. *IEEE International Symposium on Personal Indoor and Mobile Radio Communications*, 2007; 1–5.
9. Weiss T, Jondral F. Spectrum pooling: an innovative strategy for the enhancement of spectrum efficiency. *IEEE Communications Magazine* 2004; **42**(3):S8–S14.
10. Mahmoud H, Yucek H, Arslan H. OFDM for cognitive radio: merits and challenges. *IEEE Wireless Communications Magazine* 2009; **16**(2):6–15.
11. Azarnasab E, Kempter N, Patwari N, Farhang-Boroujeny B. Filterbank multicarrier and multicarrier CDMA for cognitive radio systems. *IEEE CrownCom*, 2007; 472–481.
12. Wu Z, Ratazzi P, Chakravarthy VD, Hong L. Performance evaluation of adaptive non-contiguous MC-CDMA and non-contiguous CI/MC-CDMA for dynamic spectrum access. *IEEE CrownCom*, 2008; 1–6.
13. Rajabzadeh M, Khoshbin H. Receiver design for downlink MIMO MC-CDMA in cognitive radio systems. *IEEE International Symposium on Personal Indoor and Mobile Radio Communications*, 2010; 785–789.

DOI: 10.1002/dac

14. Yuan Z, Wyglinski AM. On sidelobe suppression for multicarrier-based transmission in dynamic spectrum access networks. *IEEE Transactions on Vehicular Technology* 2010; **59**(4):1998–2006.
15. Huang S, Hwang C. Improvement of active interference cancellation: avoidance technique for OFDM cognitive radio. *IEEE Transactions on Wireless Communications* 2009; **8**(12):5928–5937.
16. Farhang-Boroujeny B, Kempter R. Multicarrier communication techniques for spectrum sensing and communication in cognitive radios. *IEEE Communications Magazine (Special Issue on Cognitive Radios for Dynamic Spectrum Access)* 2008; **48**(4):80–85.
17. Weiss T, Hillenbrand J, Krohn A, Jondral FK. Mutual interference in OFDM-based spectrum pooling systems. *IEEE Vehicular Technology Conference*, 2004; 1873–1877.
18. Mahmoud HA, Arslan H. Sidelobe suppression in OFDM based spectrum sharing systems using adaptive symbol transition. *IEEE Communications Letter* 2008; **12**(2):133–135.
19. Cosovic I, Brandes S, Schnell M. Subcarrier weighting: a method for sidelobe suppression in OFDM systems. *IEEE Communications Letter* 2006; **10**(6):444–446.
20. Xu R, Chen M. A precoding scheme for DFT-based OFDM to suppress sidelobes. *IEEE Communications Letter* 2009; **13**(10):776–778.
21. Chen HM, Chung CD. Asymptotic spectral behavior of spectrally precoded OFDM signal with arbitrary input statistics. IEEE. *Communications Letters* 2009; **13**(5):324–326.
22. Beek JVD. Sculpting the multicarrier spectrum: a novel projection precoder. *IEEE Communications Letter* 2009; **13**(12):881–883.
23. Brandes S, Cosovic I, Schnell M. Reduction of out-of-band radiation in OFDM systems by insertion of cancellation carriers. *IEEE Communications Letter* 2006; **10**(6):420–422.
24. Mahmoud HA, Arslan H. Spectrum shaping of OFDM-based cognitive radio signals. *IEEE Radio and Wireless Symposium*, 2008; 113–116.
25. Qu D, Wang Z, Jiang T. Extended active interference cancellation for sidelobe suppression in cognitive radio OFDM systems with cyclic prefix. *IEEE Transactions on Vehicular Technology* 2010; **59**(4):1689–1695.
26. Lin YP, Phoong SM. OFDM transmitters: analog representation and DFT-based implementation. *IEEE Transactions on Signal Processing* 2003; **51**(9):2450–2453.
27. Johnson R, Wichern D. *Applied Multivariate Statistical Analysis*. Prentice-Hall: Upper Saddle River, 2002.
28. Parlett NB. *The Symmetric Eigenvalue Problem.* Number 20 in Classics in Applied Mathematics. SIAM Press: Philadelphia, 1998.
29. Golub GH, Loan CFV. *Matrix Computations*. Johns Hopkins University Press: Baltimore(MD), USA, 1996.
30. Oh DC, Lee YH. Cooperative spectrum sensing with imperfect feedback channel in the cognitive radio systems. *International Journal of Communication Systems* 2010; **23**(6-7):763–779.
31. Hara S, Prasad R. Overview of multicarrier CDMA. *IEEE Communications Magazine* 1997; **35**(12):126–133.
32. Hassan ES, Zhu X, El-Khamy SE, Dessouky MI, El-Dolil SA, El-Samiel FEA. Performance evaluation of OFDM and single-carrier systems using frequency domain equalization and phase modulation. *International Journal of Communication Systems* 2011; **24**(1):1–13.

AUTHORS' BIOGRAPHIES

Morteza Rajabzadeh received his BSc and MSc degrees (both with honors) in Electrical Engineering in 2005 and 2008, respectively, from Ferdowsi University, Mashhad, Iran. At present, he is a PhD candidate at the Department of Electrical and Computer Engineering, Ferdowsi University, Mashhad, Iran. His research interests include multicarrier techniques, MIMO, code division multiple access systems and cognitive radio networks.

Hossein Khoshbin received his BSc degree in Electronics Engineering and his MSc degree in Communications Engineering in 1985 and 1987, respectively, both from Isfahan University of Technology, Isfahan, Iran. He received his PhD degree in Communications Engineering from the University of Bath, UK, in 2000. He is currently an assistant professor at the Department of Electrical and Computer Engineering, Ferdowsi University, Mashhad, Iran. His research interests include communication theory and digital and wireless communications.

DOI: 10.1002/dac